Photoinduced Electron Transfer between Chlorophyll *a* and Gold Nanoparticles

Saïd Barazzouk,[†] Prashant V. Kamat,[‡] and Surat Hotchandani*[,†]

Groupe de Recherche en Biologie Végétale, Université du Québec à Trois-Rivières, Trois-Rivières, Qc, G9A 5H7, Canada, and Notre Dame Radiation Laboratory, University of Notre Dame, Notre Dame, Indiana 46556

Received: August 5, 2004; In Final Form: September 28, 2004

Excited-state interactions between chlorophyll *a* (Chl*a*) and gold nanoparticles have been studied. The emission intensity of Chl*a* is quenched by gold nanoparticles. The dominant process for this quenching has been attributed to the process of photoinduced electron transfer from excited Chl*a* to gold nanoparticles, although because of a small overlap between fluorescence of Chl*a* and absorption of gold nanoparticles, the energy-transfer process cannot be ruled out. Photoinduced electron-transfer mechanism is supported by the electrochemical modulation of fluorescence of Chl*a*. In absence of an applied bias, Chl*a* cast on gold film, as a result of electron transfer, exhibits a very weak fluorescence. However, upon negatively charging the gold nanocore by external bias, an increase in fluorescence intensity is observed. The negatively charged gold nanoparticles create a barrier and suppress the electron-transfer process from excited Chl*a* to gold nanoparticles, resulting in an increase in radiative process. Nanosecond laser flash experiments of Chl*a* in the presence of gold nanoparticles and fullerene (C_{60}) have demonstrated that Au nanoparticles, besides accepting electrons, can also mediate or shuttle electrons to another acceptor. Taking advantage of these properties of gold nanoparticles, a photoelectrochemical cell based on Chl*a* and gold nanoparticles is constructed. A superior performance of this cell compared to that without the gold film is due to the beneficial role of gold nanoparticles in accepting and shuttling the photogenerated electrons in Chl*a* to the collecting electrode, leading to an enhancement in charge separation efficiency.

Introduction

The central issue in photosynthesis is the process of light-induced charge separation whereby light energy is converted into chemical energy by green plants. The principal pigment in this transduction of energy is chlorophyll *a* (Chl*a*). The essential roles of Chl*a* are to capture solar energy, transfer the excitation energy to special locations, the reaction centers, and bring about the charge separation for the subsequent electron-transfer processes.[1−5] The photochemical and photophysical properties of Chl*a* have, thus, been widely investigated in various laboratories around the world.[6−14]

Of particular interest has been the study of donor−acceptor systems containing Chl*a* that can mimic the photoinduced electron-transfer process of natural photosynthesis. In this regard, Chl*a*-quinones, as donor−acceptor systems, have been widely studied as simple photosynthetic models.[15−23] A reduced fluorescence quantum yield or lifetime, or a decreased triplet quantum yield of the donor, suggests that the electron transfer occurs from an excited donor. Further, the detection of cation radical of the donor and anion radical of the acceptor provides additional proof of the electron-transfer process.

The ability of Chl*a* to donate electrons from its singlet and triplet state to different quinones has been clearly demonstrated by various authors using fluorescence,[15a,e,20−23] laser photolysis,[15b−d,16a−d,19] and electron spin resonance techniques.[16a,d,e,17,18] A few years ago, photoinduced electron transfer between Chl*a* and fullerenes (known for being good electron acceptors), using nanosecond laser photolysis, was reported by El-Khouly et al.[24] While the cation radical of Chl*a*, because of its overlapping absorption with Chl*a* triplet, was not detected, the authors did observe the anion radical of fullerene.

Recently, gold nanoparticles have been drawing a lot of attention because of their unique optical and electronic properties.[25−42] Electrochemical studies have demonstrated the electron-storing properties of gold nanoparticles and their ability to act as an electric relay on a nanotemplate structure.[25a,b,26,27] Further, photochemical and spectroelectrochemical experiments have shown that gold nanoparticles capped with organic molecules exhibit unusual redox activity by readily accepting electrons from a suitable donor.[28a,b,37] Several examples of excited-state quenching by metal nanoparticles have also been reported.[38−41] Murray and co-workers have reported quenching of fluorescein and dansyl fluorophores attached to monolayer-protected gold clusters.[25c,g] The fluorescence of lissamine dye molecules attached to gold nanoparticles is strongly quenched[41] and so is the fluorescence of conjugated polymers in the presence of gold nanoparticles.[42] Fluorescence quenching in fluorophores bound to gold nanoparticles, as a result of electron transfer from excited fluorophore to gold nanoparticles, has been recently reported by us.[28a,b]

In the present work, effort has been made to probe the excited-state interactions between Chl*a* and gold nanoparticles. The objective of the study was to see if photoinduced electron transfer occurred between Chl*a* and gold nanoparticles. Fluorescence, electrochemical modulation of fluorescence, and nanosecond laser photolysis studies of Chl*a* in the presence of gold nanoparticles have been carried out to better understand the process of electron transfer from excited Chl*a* to Au nanoparticles. In addition, laser photolysis of Chl*a* in the

* To whom correspondence should be addressed. E-mail: hotchand@uqtr.ca.
[†] Université du Québec à Trois-Rivières.
[‡] University of Notre Dame.

10.1021/jp046474s CCC: $30.25
Published on Web 12/18/2004

presence of Au nanoparticles and an extra electron acceptor such as C_{60} was also performed. It is seen that Au nanoparticles can also mediate or shuttle electrons from excited Chl*a* to C_{60}. Finally, we have constructed a photoelectrochemical cell using Chl*a* film cast on a nanostructured gold electrode. A superior photoelectrochemical response of Chl*a* cast on a nanostructured gold electrode compared to that without the gold film demonstrates the beneficial role of gold nanoparticles in promoting charge separation due to their electron accepting and shuttling capability.

Experimental Section

Materials and Methods. Chl*a*, hydrogen tetrachloroaurate trihydrate, Ti(IV) isopropoxide, lithium perchlorate, lithium iodide, iodine, isooctane, and toluene, of the purest quality available, were purchased from Aldrich Chemical Co. and were used as received. Optically transparent electrodes (OTE) were cut from an indium tin oxide coated glass plate (1.3-mm thick, 20 Ω/□) obtained from Pilkington Glass Co., Toledo, OH. TiO_2 colloidal solution was prepared as reported earlier.[43]

Synthesis of Au Nanoparticles. The procedure for preparing underivatized colloidal gold nanoparticles in an organic medium is a modified version[28f] of that proposed by Brust et al.[29a] without the addition of thiol. Briefly, Au nanoparticles were prepared using a biphasic reduction procedure. A 30 mM solution of $HAuCl_4$ was transferred from aqueous phase into toluene by complexing with a phase-transfer catalyst, tetraoctylammonium bromide (TOAB, 0.1 M). The metal ions in toluene were reduced by the addition of $NaBH_4$ (0.4 M) solution dropwise. The Au colloidal suspension was dried with Na_2SO_4. The final concentration of Au nanoparticles as estimated on the basis of atomic concentration was 13 mM.[28h] The TEM micrographs of these Au nanoaprticles revealed an average particle diameter of 8 nm.

Preparation of OTE/TiO_2, OTE/Au, and OTE/TiO_2/Au Electrodes. A small aliquot (0.10 mL) of TiO_2 colloidal suspension was applied to the conducting surface of 0.8 × 2 cm^2 of OTE and was dried in air. The TiO_2 colloid-coated OTE was then annealed for 1 h at 673 K. This electrode will be referred to as OTE/TiO_2. For preparation of OTE/Au and OTE/TiO_2/Au electrodes, nanostructured gold film was electrodeposited, respectively, on OTE and OTE/TiO_2 electrodes as described earlier.[28e]

Modification of the Electrodes with Chl*a*. (i) For spectroelectrochemical (electrochemical modulation of fluorescence) measurements: Since direct adsorption of Chl*a* on OTE or OTE/Au surface was quite weak, the technique of electrodeposition as described by Tang and Albrecht[11a] was employed to deposit Chl*a* on these electrodes.

(ii) For photoelectrochemical measurements: The electrodes OTE/TiO_2 and OTE/TiO_2/Au were modified with Chl*a* by dipping them directly in isooctane solution of Chl*a*, $\sim 10^{-5}$ M, for a period of 10−12 h. The electrodes were then thoroughly washed with isooctane and used in photoelectrochemical measurements. The green coloration of the electrodes confirmed the adsorption of Chl*a*. OTE/TiO_2 electrode showed a deeper green coloration than OTE/TiO_2/Au electrode, indicating a stronger adsorption of Chl*a* on TiO_2 nanoparticles than on Au nanoparticles.

Chl*a* modified electrodes will be denoted, hereafter, as OTE/Chl*a*, OTE/Au/Chl*a*, OTE/TiO_2/Chl*a*, and OTE/TiO_2/Au/Chl*a*.

Absorption and Fluorescence Measurements. Absorption spectra were recorded with a Cary 50 spectrophotometer. The emission spectra of the solutions and the films were recorded with an SLM S-8000 photocounting spectrophotometer. Fluorescence from films was monitored in a front-face geometry.

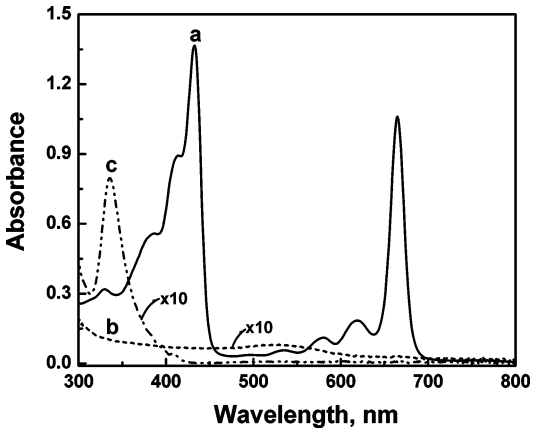

Figure 1. Absorption spectra of toluene solutions of (a) 14 μM Chl*a*, (b) 28 μM Au nanoparticles, and (c) 1.38 μM C_{60}.

Spectroelectrochemical and Photoelectrochemical Measurements. The measurements were carried out in a thin layer cell consisting of a 5-mm path length quartz cuvette with two sidearms attached for inserting reference (SCE) and counter (Pt gauze) electrodes. The description of the cell can be found elsewhere.[44] The design of the cell is such that it can be inserted into the sample compartment of an emission spectrophotometer (SLM S-8000) and can carry out the measurements under the influence of an applied bias. A Princeton Applied Research (PAR) model 173 potentiostat and model 175 Universal Programmer were used in biasing the electrodes.

Photocurrent and photovoltage were measured with Keithley, Model 617, programmable electrometer. A collimated light beam from a 250 W xenon lamp was used as the light source. A Baush and Lomb high-intensity grating monochromator was introduced into the path of the excitation beam for selecting the excitation wavelengths. The active area of the electrode was 1 cm^2 and was illuminated through the back OTE face.

Nanosecond Laser Flash Photolysis. Nanosecond laser flash photolysis experiments were performed using a 532-nm (second-harmonic) laser pulse (~6 ns pulse width) from a Quanta Ray model CDR-1 Nd:YAG laser system for excitation. The laser output was suitably attenuated to about 2 mJ/pulse and defocused to minimize the multiphoton process. The experiments were performed in a rectangular quartz cell of 6-mm path length with a right angle configuration between the direction of laser excitation and analyzing light.[45] The photomultiplier output was digitized with a Tektronix 7912 AD programmable digitizer. The solutions were deaerated by purging with nitrogen gas. A typical experiment consisted of a series of two to three replicate shots/single measurement. The average signal was processed with a LeCroy digitizer.

Results and Discussions

Absorption Characteristics. Figure 1 presents the absorption spectra of Chl*a*, gold nanoparticles, and C_{60} in toluene. The principal absorption peaks of chlorophyll (spectrum a) in the red at 665 nm, Q-band, and at 433 nm in the blue, Soret band, are in agreement with those reported in the literature,[46] and Chl*a* is present in monomeric form. The 530-nm absorption band (spectrum b) is characteristic of the surface palsmon band of gold nanoparticles. C_{60} has a weak absorption in the visible region at 404 nm and a strong one in the UV around 329 nm (spectrum c).

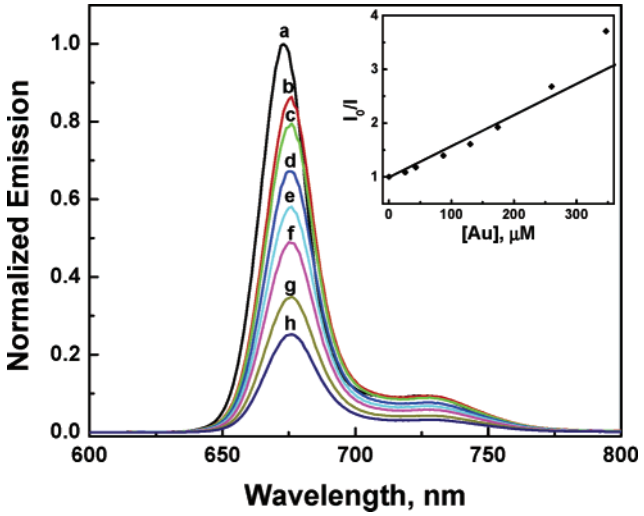

Figure 2. Emission spectra of 5.25 μM Chl*a* in toluene recorded in the presence of different concentrations of Au nanoparticles: (a) 0, (b) 26, (c) 43, (d) 87, (e) 130, (f) 174, (g) 260, and (h) 347 μM. Excitation wavelength was 433 nm. The insert shows Stern−Volmer plot of the quenching of Chl*a* by gold nanoparticles. The fluorescence intensity was monitored at 675 nm.

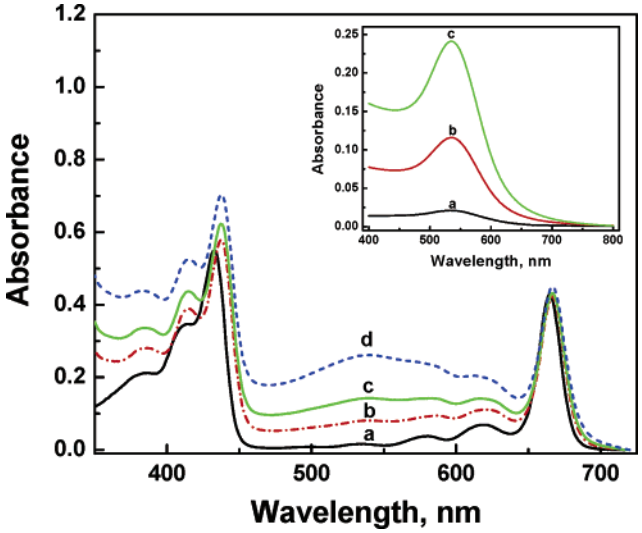

Figure 3. Absorption spectra of toluene solutions of 5.25 μM Chl*a* in the presence of different concentrations of Au nanoparticles: (a) 0, (b) 37.5, (c) 75, and (d) 150 μM. The inset shows the absorption spectra of different concentration of Au nanoparticles in toluene: (a) 22, (b) 150, and (c) 300 μM.

Fluorescence Quenching of Chl*a* by Gold Nanoparticles. In Figure 2 are displayed the fluorescence spectra of Chl*a* in toluene in the presence of varying concentration of gold nanoparticles. The fluorescence of Chl*a* in toluene exhibits a maximum at ~675 nm (spectrum a), which is characteristic of emission from monomeric Chl*a* in nonpolar solvent. Upon addition of gold nanoparticles, one observes a progressive quenching of the fluorescence of Chl*a* with increasing amounts of Au nanoparticles. The samples were prepared by injecting microliter quantities of Au nanoparticles (13 mM) into 3 mL of Chl*a* solution (5.25 μM) in toluene.

The quenching follows the Stern−Volmer relation $I_0/I = 1 + K_{SV}[Q]$, where I_0 and I are the emission intensities of Chl*a* in absence and presence of quencher Q (gold nanoparticles), respectively, K_{SV} is the Stern−Volmer quenching constant, and [Q] is the concentration of the quencher. The plot is linear in the concentration range of 300 μM of gold nanoparticles. Higher concentrations (>300 μM) of Au nanoparticles due to their appreciable absorbance of 433-nm excitation wavelength were avoided. From the slope of the plot, a value of $\sim 10^4$ is obtained for K_{SV}. Similar results for the quenching of Chl*a* by Au nanoparticles were also obtained by using excitation wavelength of 655 nm.

The quenching can be both static and dynamic. The former involves the formation of a nonfluorescent complex between the fluorophore and quencher in their ground states, whereas the latter requires diffusive encounters between fluorophore and quencher during the lifetime of the excited state of the fluorophore. In both cases, Stern−Volmer plots (I_0/I vs [Q]) are linear. In static quenching, the quenching constant K_{SV} is the association constant,[47] while in the dynamic quenching, K_{SV} represents the product of bimolecular quenching rate constant, k_q, and fluorescence lifetime, τ_0, of the fluorophore in the absence of quencher, that is, $K_{SV} = k_q\tau_0$. In solution, where both fluorophore and quencher can move freely, the value of k_q approaches that of a diffusion-controlled rate constant k_d, ($k_d = 8RT/3000\eta$ for a bimolecular process, where R is the gas constant, T is the temperature, and η is the viscosity of the solvent). k_d, depending upon the viscosity of solvent, has a value in the range of 10^9-10^{10} M^{-1} s^{-1}.

Assuming that the deactivation of the excited Chl*a* occurs by collisions with the quencher in fluid solution (dynamic quenching), the value of k_q ($=K_{SV}/\tau_0$), taking fluorescence lifetime of Chl*a* in absence of gold nanoparticles as 5.6 ns (determined experimentally from the decay−time profile of the emission of Chl*a*) into account, is calculated to be 1.37×10^{12} M^{-1} s^{-1}. This value is much higher than the diffusion-controlled rate constant, k_d, which is 5×10^9 M^{-1} s^{-1} with toluene as a solvent in the present case ($\eta_{toluene} = 1.07$ cP at 25 °C). Thus, a 3 orders of magnitude larger value of k_q than k_d, coupled with a small decrease in fluorescence lifetime of Chl*a* from 5.6 ns (in absence of gold nanoparticles) to 3.9 ns in the presence of gold nanoparticles (300 μM), and the changes (5−10-nm red shift) observed in the absorption spectrum of Chl*a* in the presence of gold nanoparticles (Figure 3) suggest that static quenching plays a major role in the quenching of the fluorescence of Chl*a* by gold nanoparticles. The value of 10^4 for K_{SV}, thus, represents the association constant between Chl*a* and gold nanoparticles in the present case.

How Chl*a* and gold nanoparticles are associated is not clear to us at present; however, gold nanoparticles, being negatively charged because of the strong reducing agent $NaBH_4$ used in their preparation,[48] could bind to Chl*a* at central magnesium atom which is coordinatively unsaturated.[10e,f] Zero-field ODMR (optical detection of magnetic resonance) experiments have been quite helpful in elucidating the ligation state of the central magnesium atom of Chl*a*. The zero-field splitting parameter of the triplet state of Chl*a* determined by fluorescence detected ODMR of Chl*a* at 2 K has clearly shown that nucleophilic agents such as H_2O and pyridine, possessing lone pair of electrons, easily bind to magnesium atom and yield mono- and biligated species of Chl*a*.[49,50] It is thus highly likely that negatively charged gold nanoparticles are bound to the magnesium metal center of Chl*a*. Consequently, static quenching will play a major role in the quenching of Chl*a* fluorescence by gold nanoparticles, explaining the high value of K_{SV}. Enormously high values of K_{SV} for the fluorescence quenching of cationic conjugated polymers by gold nanoparticles have also been attributed, in part, to the static quenching by Heeger and co-workers.[42]

In general, there are several important molecular processes whereby a quencher can deactivate an excited fluorophore. Important ones are those of the electron transfer and energy transfer. Various examples in the literature in which the excited-state quenching has been attributed to energy transfer to gold nanoparticles have been reported.[25c,g,38,39] However, since metals in nanoparticle dimensions are more electronegative than the bulk material, they can also participate in electron-transfer process. Electrochemical studies have shown that gold nanoparticles can accept and store electrons.[25a,b,37a] Our recent study has shown the possibility of achieving a photoinduced electron transfer from excited pyrene to gold in colloidal suspension of pyrenethiol-functionalized gold nanoparticles.[28a,b] Thus, it is very likely that electron transfer is the dominant process in the emission quenching of Chl*a* by gold nanoparticles where excited Chl*a* donates electrons to gold nanoparticles. This is based on the fact that the difference between the oxidation potential of Chl*a** (∼−1.1 V vs NHE)[51] and the Fermi level of Au (∼+0.5 V vs NHE) provides the necessary driving force for such a charge-transfer process. A large value of association constant (10^4 M^{-1}), indicating a strong binding between Chl*a* and gold nanoparticles, also provides favorable conditions for the heterogeneous charge-transfer process at Chl*a*−Au nanoparticles interface.

If indeed gold nanoparticles act as electron acceptors, it should be possible to modulate the electron-transfer quenching of excited fluorophore by charging the gold nanoparticles at an electrode surface by an electrochemical bias and, effectively, observe an enhancement in fluorescence of the fluorophore upon negatively charging the Au nanoparticles.

Electrochemical Modulation of Chl*a* Emission. To investigate the influence of charging the gold nanocore on the Chl*a* fluorescence, the fluorophore (Chl*a*) was deposited on a nanostructured gold electrode, OTE/Au, by electrodeposition technique.[11a] This electrodeposition method was necessary as the direct adsorption of Chl*a* on OTE or OTE/Au electrodes was very weak. Electrodeposited Chl*a* has absorption and fluorescence maxima in the red at ∼740 and 750−760 nm, respectively.[8f,11a] The electrode OTE/Au/Chl*a* was installed in a thin layer cell and placed in the compartment of the fluorimeter. An electrochemical bias was applied to the electrode and fluorescence (in a front-face configuration) was recorded. Figure 4 shows the emission spectra of Chl*a* deposited on gold film (OTE/Au/Chl*a*) under different applied negative potentials. As a reference, fluorescence of Chl*a* deposited on plain OTE is also shown (spectrum g); one can see quite a strong fluorescence of Chl*a* with a maximum at ∼750 nm. As far as the fluorescence of Chl*a* deposited on nanostructured gold electrode, OTE/Au, is concerned, it is almost totally quenched (spectrum a). The quenching is the result of an additional pathway of electron transfer for the decay of Chl*a** on gold film besides the already existing radiative and nonradiative deactivation modes. That the quenching is indeed due to the electron-transfer process is evident from the modulation of the fluorescence by the electrochemical bias (spectra b−f).

Application of a positive bias to the electrode neither restores nor further quenches the fluorescence. However, by biasing the electrode to negative potentials, an increase in fluorescence intensity is observed (spectra b−f). The overall shape of the emission band essentially remains the same. This suggests that the photoactive fluorescing species that contributes to the emission remains unperturbed. As we bias the electrode to negative potentials, the gold particles become negatively charged and repel the electrons from excited Chl*a*. This suppresses the

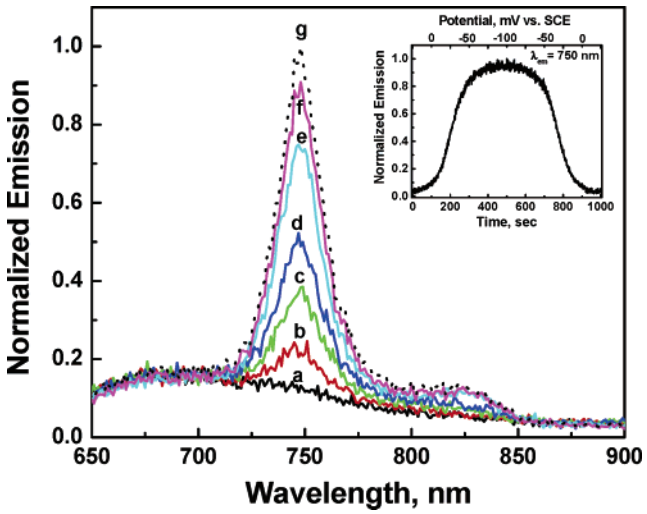

Figure 4. Emission spectra of OTE/Au/Chl*a* at different negative applied potentials: (a) 0, (b) −20, (c) −40, (d) −60, (e) −80, and (f) −100 mV. Spectrum g is the emission of Chl*a* deposited on plain OTE. Excitation wavelength: 433 nm. The electrode was maintained at a set negative potential vs SCE (electrolyte: 0.1 M lithium perchlorate in deionized water) for 3 min before recording the individual emission spectrum. Insert shows the fluorescence response of OTE/Au/Chl*a* at 750 nm during two electrochemical scans.

SCHEME 1: Electron Transfer Dynamics and Fluorescence of Chl*a* Bound to Au Nanoparticles before and after Charging of Gold Nanoparticles

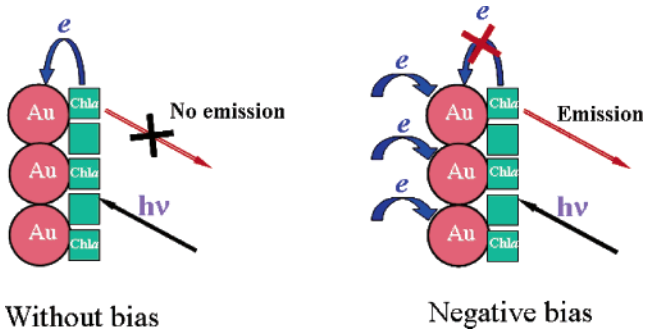

electron-transfer process from excited Chl*a* to gold nanoparticles, which, in turn, leads to an increase in radiative charge recombination, resulting in an enhancement of the fluorescence. At potentials around −100 mV, electron transfer from Chl*a** to gold seems to be completely suppressed, and we achieve a saturation in emission increase (spectrum f). More than 90% of the quenched emission is restored. The quenching was again observed by reversing the potential to the lower values of negative biases. This discharges the gold nanocore and reactivates the process of electron transfer from excited Chl*a* to gold nanoparticles. The reversibility of fluorescence quenching/restoration with applied bias during an electrochemical scan is shown in the inset of Figure 4. The scan rate of potential was kept at its minimum value of 1 mV/s so that the charges have enough time to equilibrate and respond to applied potentials.

Scheme 1 illustrates the influence of the charging of gold nanocore with negative electrochemical bias on electron-transfer and fluorescence behavior of Chl*a* deposited on a nanostructured gold film. Similar observations have also been made with pyrenethiol deposited on a gold film.[28b]

Biasing the OTE/Au/Chl*a* electrode to negative potentials did not cause any deterioration or desorption of Chl*a*. This was verified by checking the emission of the electrolyte solution after removing the electrode from the cell; effectively no

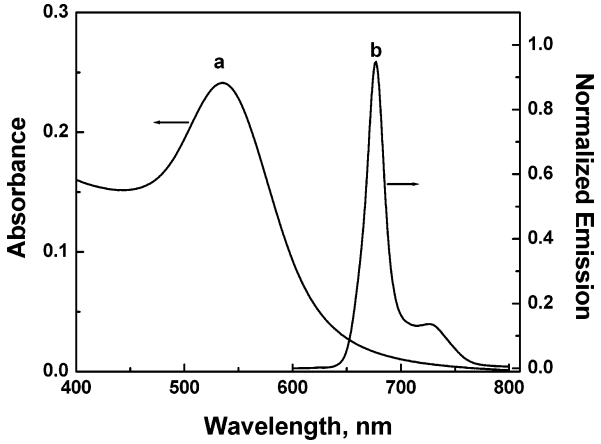

Figure 5. (a) Absorption spectrum of 300 μM Au nanoparticles in toluene and (b) emission spectrum of 5.25 μM Chl*a* in toluene (excitation wavelength: 433 nm).

emission was detected. Further, the absorption spectrum of the electrode recorded after these spectroelectrochemical experiments also did not indicate any deterioration of the film. Applying negative biases to Chl*a* deposited on plain OTE without the gold film, that is, the OTE/Chl*a* electrode, had no effect on the fluorescence of Chl*a*. These results confirm that an externally applied electrochemical bias modulates the electron-transfer dynamics between Chl*a** and gold nanoparticles and that the quenching in fluorescence of Chl*a* is due to the electron transfer from excited Chl*a* to gold nanoparticles. However, because of a small overlap between the fluorescence of Chl*a* and absorption of gold nanoparticles (Figure 5), energy transfer via both short-range Dexter and long-range Förster mechanisms cannot be ruled out. The role of long-range energy-transfer process was also invoked by Heeger and co-workers in the fluorescence quenching of cationic polymers by gold nanoparticles.[42]

Laser Photolysis Experiments. To further probe the involvement of gold nanoparticles in electron-transfer process, we have carried out nanosecond laser photolysis study. The transient absorption spectra recorded after 7 μs following 532-nm laser excitation (pulse width of ~6 ns) of the deoxygenated Chl*a* alone and in the presence of Au nanoparticles or C_{60} in toluene are shown in Figure 6. Using 532-nm laser light, we are predominantly exciting Chl*a* (14 μM) since its absorption is much higher than that of Au nanoparticles (28 μM) and C_{60} (1.38 μM) at this wavelength (Figure 1). The transient absorption of Chl*a* alone shows a band characteristic of its excited triplet around 460 nm and two absorption bleaching bands assigned to its ground state at 443 and 665 nm (spectrum a, Figure 6A). The lifetime of ^{3}Chl*a** evaluated from the decay−time profile monitored at 460 was 65 μs, which is in agreement with the value reported previously.[52,53] In their recent work, El-Khouly et al.[24] reported a lifetime of 35 μs for ^{3}Chl*a** in benzonitrile. This decrease in the lifetime value is possibly due to the high concentration of Chl*a* used by this group (100 μM) leading probably to a triplet−triplet annihilation process and is also due to a different (polar) solvent used.

The transient absorption spectrum of Chl*a* and Au nanoparticles (spectrum b, Figure 6A) shows almost the same transient spectral features as that of Chl*a* alone but the lifetime of ^{3}Chl*a** in this case decreased to 49 μs, and an increase in absorbance (ΔA) between 450 and 600 nm was also observed. This decrease in lifetime is indicative of an electron-transfer process from ^{3}Chl*a** to adjacent Au nanoparticles, supposedly leading to the

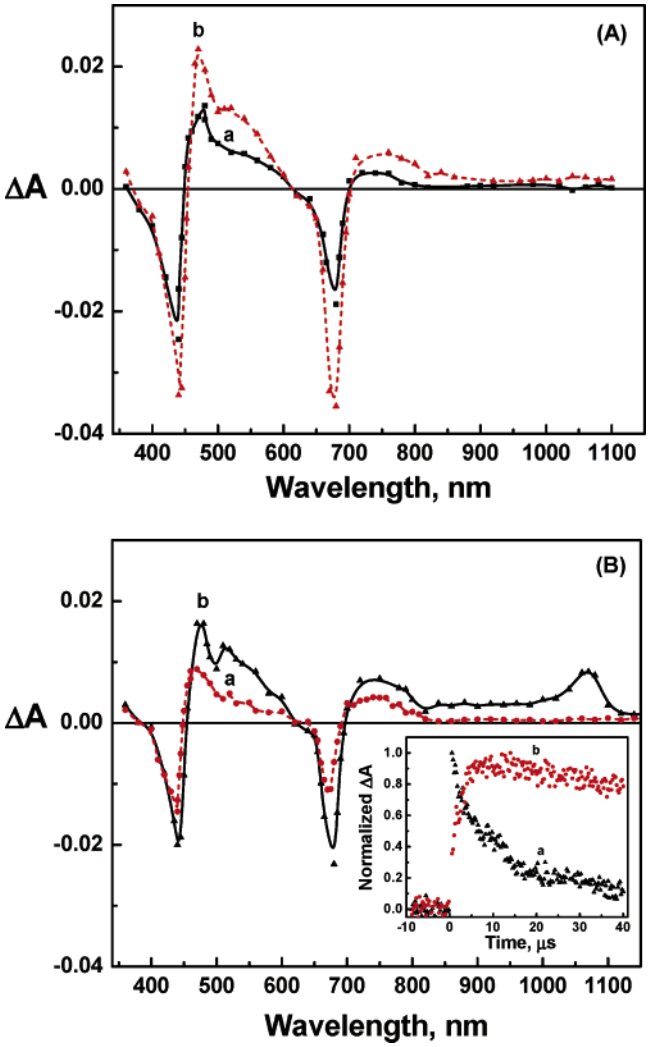

Figure 6. (A) Transient absorption spectra recorded 7 μs after the laser flash (532 nm) of toluene solutions of (a) 14 μM Chl*a* and (b) Chl*a* (14 μM) + 28 μM gold nanoparticles. (B) Transient absorption spectra recorded 7 μs after the laser flash of toluene solutions of (a) Chl*a* (14 μM) + 1.38 μM C_{60} and (b) Chl*a* (14 μM) + Au (28 μM) + C_{60} (1.38 μM). The insert shows (a) the decay−time profile monitored at 460 nm and (b) the growth−time profile monitored at 1070 nm, for Chl*a* + Au + C_{60}. The laser excitation wavelength was 532 nm.

formation of Chl*a* cation radical (eq 2) with a characteristic absorption in 450−600-nm region

$$\text{Chl}a + h\nu \rightarrow {}^1\text{Chl}a^* \rightarrow {}^3\text{Chl}a^* \quad (1)$$

$$^3\text{Chl}a^* + \text{Au} \rightarrow \text{Chl}a^{+\bullet} + \text{Au}(e^-) \quad (2)$$

Unfortunately, like many other research groups, we have failed to resolve the transient absorption band of Chl$a^{+\bullet}$ in the visible region which lies in the same region where ^{3}Chl*a** absorbs strongly. However, the observed increase in ΔA between 450 and 600 nm is an indirect evidence of the presence of Chl$a^{+\bullet}$. We, next, conducted the same photolysis experiment of Chl*a* but in the presence of a well-known electron acceptor C_{60} (1.38 μM). However, we got the same result (spectrum a, Figure 6B) as that for Chl*a* and Au nanoparticles: neither Chl*a* cation radical, because of its overlapping absorption with ^{3}Chl*a**, nor C_{60} anion radical (products of electron transfer between ^{3}Chl*a** and C_{60}) was observed. While anion radical of C_{60} absorbing at 1070 nm has recently been reported by El-Khouly et al. in their experiments with Chl/C_{60} system (with C_{60} concentration

SCHEME 2: Electron Transfer between Chl*a, Au Nanoparticles, and C_{60}**

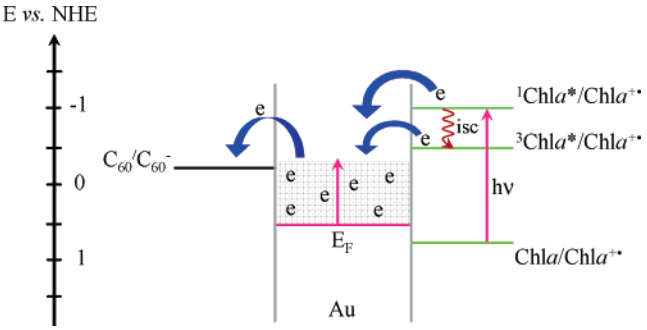

of 0.1 mM),[24] we, however, because of the lower concentration of C_{60} (1.38 μM) used in our experiments, could not detect the anion radical of C_{60}, although a decrease in the lifetime of ^{3}Chl*a** was observed (40 μs). The absence of the C_{60} anion radical is probably due to its quick recombination reaction with Chl*a* cation radical.

The photolysis of Chl*a* was again carried out but this time in the presence of both Au nanoparticles and C_{60}. The transient absorption spectrum (spectrum b, Figure 6B) shows, in addition to the spectral features of ^{3}Chl*a**, a new transient absorption band at 1070 nm which is characteristic of C_{60} anion radical. The appearance of the anion radical of C_{60} in this case is mainly due to the role of Au nanoparticles in accepting and shuttling the electrons from the excited Chl*a* to C_{60}. In other words, the formation of $C_{60}^{-\bullet}$ is via an electron-transfer process from Chl*a** to C_{60} assisted by Au nanoparticles acting as electron mediators as shown in eq 3, since Chl*a* and C_{60} alone did not show any anion radical of C_{60}.

$$^3\text{Chl}a^* + \text{Au} + C_{60} \rightarrow \text{Chl}a^{+\bullet} + \text{Au}(e^-) + C_{60} \rightarrow \text{Chl}a^{+\bullet} + \text{Au} + C_{60}^{-\bullet} \quad (3)$$

Scheme 2 further illustrates this process of electron transfer mediated by Au nanoparticles. Excited Chl*a*, being at a higher energy level (^{1}Chla* ~ -1.1 V and ^{3}Chla* ~ -0.65 vs NHE),[51] transfers electrons to the gold nanoparticles. The electron accumulation in gold nanoparticles raises the Fermi level of Au to more negative potentials until it reaches the energy level of C_{60} leading to a quick transfer of electrons to C_{60} which continues until an equilibrium is established between Au and C_{60}/C_{60}^- redox couple. The ability of gold nanoparticles in storing and shuttling of electrons has been described by charging effects[25a,b] and Fermi-level equilibration in semiconductor-gold nanostructures.[28f−h,37a] The electron accepting and shuttling character of gold nanoparticles has also been recently demonstrated by Kamat and co-workers[28f,h] in their work with TiO_2-Au-C_{60} system, where Au accepts electrons from illuminated TiO_2 and delivers them to C_{60}.

The inset of Figure 6B shows the decay of the ^{3}Chl*a** transient absorption at 460 nm and the growth of $C_{60}^{-\bullet}$ absorption at 1070 nm in Chl*a*−Au−C_{60} system with a similar first-order kinetics with lifetimes of 37 and 42 μs, respectively. This confirms the interaction between ^{3}Chl*a** and C_{60} via Au.

Photocurrent Generation Efficiency. The ability of gold nanoparticles to accept and shuttle electrons from excited fluorophores suggests that it is possible to obtain a better charge separation in gold nanocore−fluorophore assemblies and employ them to improve the energy conversion efficiencies of photoelectrochemical solar cells. We have thus constructed a photoelectrochemical cell using an Au modified Chl*a* film as a photoanode. Figure 7A shows the incident photon-to-charge carrier generation efficiency (IPCE) of Chl*a* film cast on TiO_2 and TiO_2/Au nanostructured electrodes. A nearly 4 times higher IPCE at 440 nm can be easily noticed in the system with the gold film, that is, OTE/TiO_2/Au/Chl*a*, (spectrum b), than that without the gold film (spectrum a). The qualitative matching of the action spectra with absorption spectrum of Chl*a* (spectrum c) suggests that photocurrent generation originates in the excitation of Chl*a*. Blank experiments conducted with OTE/TiO_2 and OTE/TiO_2/Au electrodes did not produce detectable photocurrent in the visible region. The mechanism of photocurrent generation in an OTE/TiO_2/Au/Chl*a* electrode is depicted in Scheme 3; the use of redox couple I_3^-/I^- is to regenerate the original sensitizer (Chl*a*).

The absorbance of OTE/TiO_2/Au/Chl*a* electrode in blue and red wavelength regions, because of the poor adsorption of Chl*a* on Au, is actually inferior to that for OTE/TiO_2/Chl*a* (as mentioned in Experimental Section, a deeper green coloration of OTE/TiO_2/Chl*a* electrode than that of OTE/TiO_2/Au/Chl*a* suggests a higher absorbance of OTE/TiO_2/Chl*a*). Since IPCE

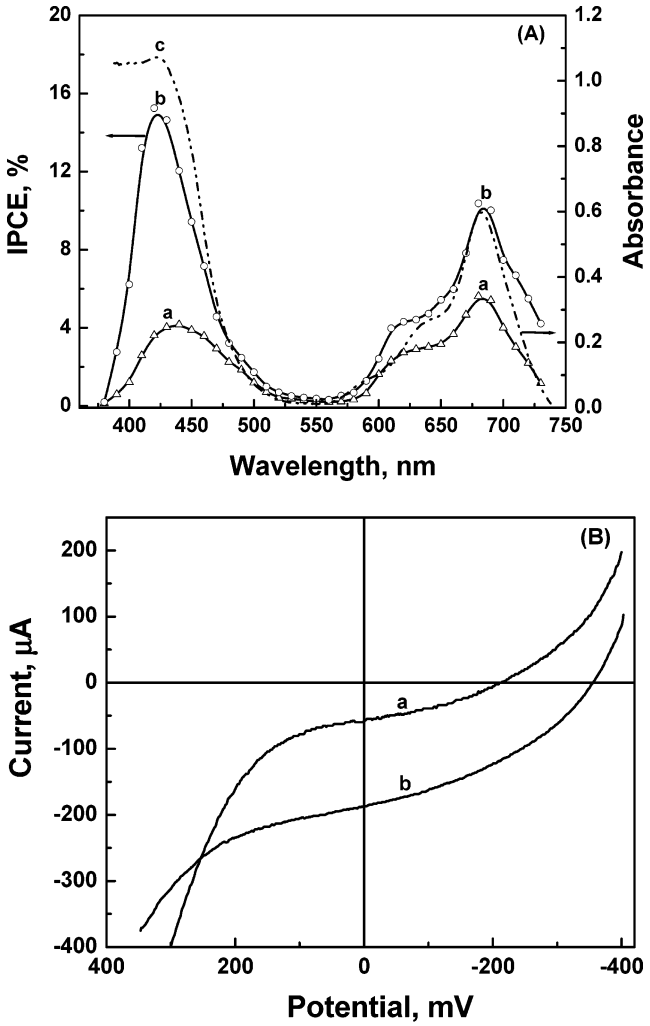

Figure 7. (A) Photocurrent action spectra of (a) OTE/TiO_2/Chl*a* and (b) OTE/TiO_2/Au/Chl*a* electrodes. IPCE(%) was determined using equation IPCE(%) = $(1240/\lambda)(i_{sc}/I_{inc}) \times 100$, where i_{sc} (mA/cm^2) is the short circuit photocurrent and I_{inc} (mW/cm^2) is the incident light intensity. Electrolyte used was 0.5 M LiI and 0.01 M I_2 in acetonitrile. Also included is the absorption spectrum of OTE/TiO_2/Chl*a* (spectrum c). (B) $I-V$ characteristics of (a) OTE/TiO_2/Chl*a* and (b) OTE/TiO_2/Au/Chl*a* electrodes under visible light illumination. Electrolyte used was 0.5 M LiI and 0.01 M I_2 in acetonitrile; counter electrode: Pt gauze; reference electrode: SCE.

SCHEME 3: Mechanism of Photocurrent Generation in the Photoelectrochemical Cell Using OTE/TiO_2/Au/Chl*a* as Photoanode

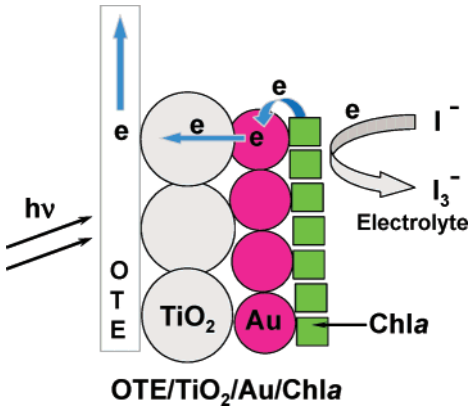

depends directly on light-harvesting efficiency (LHE) of the sensitizer, (LHE = $1-10^{-A}$, where A is the absorbance), a comparable absorbance of OTE/TiO_2/Au/Chl*a* to that of OTE/TiO_2/Chl*a* would, in fact, result in even higher IPCE (more than 4 times) for Chl*a* adsorbed on a nanostructured gold film relative to the one without the gold film. This surely suggests an improved charge separation brought about by gold nanoparticles.

The explanation is that in OTE/TiO_2/Au/Chl*a*, the gold nanoparticles after receiving electrons from Chl*a** shuttle them to TiO_2, similar to what was observed with Chl*a*−Au−C_{60} system in laser photolysis experiments described above. That is, in OTE/TiO_2/Au/Chl*a*, excited Chl*a*, being at a higher energy level (−1.1 V vs NHE), transfers electrons to the gold nanoparticles (E_F = 0.5 V vs NHE). This raises the Fermi level of Au to more negative potentials until it reaches the Fermi level of TiO_2 (−0.5 V vs NHE) whereupon a quick transfer of electrons from Au to TiO_2 takes place. As a result, the photogenerated electrons are farther apart from the holes left in Chl*a* compared to that in OTE/TiO_2/Chl*a* system and escape recombination, producing a larger photocurrent. A higher zero current potential in OTE/TiO_2/Au/Chl*a*, illustrated in Figure 7B, further proves this point. The zero current potential of TiO_2/Chl*a* film shifts from −0.21 V to −0.36 V upon modification with gold nanoparticles. This negative increase of ∼150 mV in the zero current potential is due to the presence of gold nanoparticles which facilitate electron transport between Chl*a* and TiO_2 by accepting electrons and shuttling them to TiO_2, thereby decreasing the charge recombination. Lahav et al.,[34d] in their studies of photocurrent generation in Zn−porphyrin−dyad on gold nanoparticles, have also invoked gold nanoparticles in facilitating electron−hole separation and electron transport to the collecting electrode. The beneficial role of gold nanoparticles in photocurrent generation has also been demonstrated by Kuwahara et al.[54] in tris (2,2′-bipyridine) ruthenium (II)-viologen linked thiol and by us[28c] in fullerene-functionalized gold nanoparticles.

Conclusion

The present study shows that photoinduced electron transfer occurs from excited Chl*a* to gold nanoparticles. The difference between the oxidation potential of Chl*a** and the Fermi level of Au provides the necessary driving force for such an electron-transfer process. A large value of association constant (10^4 M^{-1}), indicating a strong binding between Chl*a* and gold nanoparticles, also provides favorable conditions for the heterogeneous charge-transfer process at Chl*a*−Au nanoparticles interface. The electrochemical modulation of the emission intensity of Chl*a* further supports the electron-transfer process between excited Chl*a* and Au. Nanosecond laser flash experiments of Chl*a* in the presence of gold nanoparticles and C_{60} have demonstrated that Au nanoparticles, besides accepting electrons, can also mediate electrons to another acceptor thus aiding in charge separation. The higher photocurrent generation efficiency (IPCE) of the photoelectrochemical cell using OTE/TiO_2/Au/Chl*a* electrode compared to that without the gold film, that is, OTE/TiO_2/Chl*a*, is due to the ability of Au nanoparticles in accepting and shuttling the electrons from excited Chl*a* to TiO_2, leading to an enhancement in charge separation.

Acknowledgment. The work described herein was supported by the Natural Sciences and Engineering Research Council of Canada. P.V.K. would like to acknowledge the support of Office of the Basic Energy Science of the U.S. Department of Energy. This is contribution No. 4541 from the Notre Dame Radiation Laboratory.

Note Added after ASAP Publication. Two typographical errors were corrected: the unit Ω/Å was corrected to Ω/□, and Foster mechanisms was corrected to Förster mechanisms. This paper was published on the Web on 12/18/04. The corrected version was posted on 1/5/05.

References and Notes

(1) *The Chlorophylls*; Vernon, L. P., Seely, G. R., Ed.; Academic Press: New York, 1966.
(2) *Chlorophylls*; Scheer, H., Ed.; CRC Press: Boca Raton, FL, 1995.
(3) Parusel, A. B. J.; Grimme, S. *J. Phys. Chem.* **2000**, *104*, 5395.
(4) (a) Hurley, J. K.; Tollin, G. *Sol. Energy* **1982**, *28*, 187. (b) Tollin, G. *J. Phys. Chem.* **1976**, *80*, 2274.
(5) Van Zandvoort, M. A. M. J.; Wrobel, D.; Lettinga, P.; Van Ginkel, G.; Levine, Y. K. *Photochem. Photobiol.* **1995**, *62*, 299.
(6) (a) Bowers, P. G.; Poter, G. *Proc. R. Soc. London, Ser. A* **1967**, *296*, 435. (b) Beddard, G. S.; Carlin, S. E.; Porter, G. *Chem. Phys. Lett.* **1976**, *43*, 27. (c) Costa, S. M. De B.; Froines, J. R.; Harris, J. M.; Leblanc, R. M.; Orger, B. H.; Porter, G. *Proc. R. Soc. London, Ser. A* **1972**, *326*, 503. (d) Kelly, A. R.; Porter, G. *Proc. R. Soc. London, Ser. A* **1970**, *315*, 149.
(7) Dreuw, A.; Fleming, G. R.; Head-Gordon, M. *Phys. Chem. Chem. Phys.* **2003**, *5*, 3247.
(8) (a) Bedja, I.; Kamat, P. V.; Hotchandani, S. *J. Appl. Phys.* **1996**, *80*, 4637. (b) Hotchandani, S.; Kamat, P. V. *Chem. Phys. Lett.* **1992**, *191*, 320. (c) Kassi, H.; Hotchandani, S.; Leblanc, R. M. *Appl. Phys. Lett.* **1993**, *62*, 2283. (d) Nasr, C.; Taleb, T.; Leblanc, R. M.; Hotchandani, S. *Appl. Phys. Lett.* **1996**, *69*, 1823. (e) Taleb, T.; Nasr, C.; Hotchandani, S.; Leblanc, R. M. *J. Appl. Phys.* **1996**, *79*, 1701. (f) Boussad, S.; Hotchandani, S.; Leblanc, R. M. *Appl. Phys. Lett.* **1993**, *63*, 1768.
(9) Kusumoto, Y.; Uchikoba, M. *Chem. Lett.* **1991**, *11*, 1985.
(10) (a) Wasielewski, M. R.; Studier, M. H.; Katz, J. J. *Proc. Natl. Acad. Sci. U.S.A.* **1976**, *73*, 4282. (b) Druyan, M. E.; Norris, J. R.; Katz, J. J. *J. Am. Chem. Soc.* **1973**, *95*, 1682. (c) Cotton, T. M.; Loach, P. A.; Katz, J. J.; Ballschmiter, K. *Photochem. Photobiol.* **1978**, *27*, 735. (d) Shipman, L.; Cotton, T. M.; Norris, J. R.; Katz, J. J. *J. Am. Chem. Soc.* **1976**, *98*, 8222. (e) Katz, J. J. *CIBA Foundation Symposium 61*; Excerpta Medica: Amsterdam, 1979; p 344. (f) Evans, T. A.; Katz, J. J. *Biochim. Biophys. Acta* **1975**, *396*, 414.
(11) (a) Tang, C. W.; Albrecht, A. C. *Mol. Cryst. Liq. Cryst.* **1974**, *25*, 53. (b) Tang, C. W.; Albrecht, A. C. *J. Chem. Phys.* **1975**, *63*, 953. (c) Tang, C. W.; Albrecht, A. C. *Nature Vol.* **1975**, *254*, 507.
(12) Chapados, C. *Photochem. Photobiol.* **1988**, *47*, 115.
(13) Zigmatat, D.; Hiller, R. G.; Sundstrom, V.; Polivka, T. *PNAS* **2002**, *99*, 16760.
(14) Lawrence, M. F.; Dodelet, J.-P.; Dao, L. H. *J. Phys. Chem.* **1984**, *88*, 950.
(15) (a) Beddard, G. S.; Porter, G.; Weese, G. M. *Proc. R. Soc. London, Ser. A* **1975**, *342*, 317. (b) Darwent, J. R.; Kalyanasundaram, K.; Porter, G. *Proc. R. Soc. London, Ser. A* **1980**, *373*, 179. (c) Kelly, A. R.; Porter, G. *Proc. R. Soc. London, Ser. A* **1970**, *319*, 319. (d) Beddard, G. S.; Carlin, S.; Harris, L.; Porter, G.; Tredwell, C. J. *Photochem. Photobiol.* **1978**, *27*, 433. (e) Brown, R. G.; Harriman, A.; Porter, G. *J. Chem. Soc., Faraday Trans.* **1977**, *73*, 113. (f) Kalyanasundaram, K.; Porter, G. *Proc. R. Soc. London, Ser. A* **1978**, *364*, 29.

(16) (a) Cheddar, G.; Tollin, G. *Photobiochem. Photobiophys.* **1980**, *1*, 235. (b) Hurley, J. K.; Castelli, F.; Tollin, G. *Photochem. Photobiol.* **1980**, *32*, 79. (c) Raman, R.; Tollin, G. *Photochem. Photobiol.* **1971**, *13*, 135. (d) Cheddar, G., Castelli, F.; Tollin, G. *Photochem. Photobiol.* **1980**, *32*, 71. (e) Harbour, J. R.; Tollin, G. *Photochem. Photobiol.* **1974**, *20*, 271. (f) Tollin, G.; Castelli, F.; Cheddar, G.; Rizzuto, F. *Photochem. Photobiol.* **1978**, *29*, 147. (g) Tollin, G.; Rizzuto, F. *Photochem. Photobiol.* **1978**, *27*, 487. (h) Glen, C.; Tollin, G. *Photobiochem. Photobiophys.* **1980**, *1*, 235.

(17) Hales, B. J.; Bolton, J. R. *J. Am. Chem. Soc.* **1972**, *95*, 3314.

(18) Warden, J. J. *Isr. J. Chem.* **1981**, *21*, 338.

(19) Mathis, P.; Setif, P. *Isr. J. Chem.* **1981**, *21*, 316.

(20) Natarajan, L. V.; Ricker, J. E.; Blankenship, R. E.; Chang, R. *Photochem. Photobiol.* **1984**, *3*, 301.

(21) Rajagopal, S.; Egorova, E. A.; Bukhov, N. G.; Carpentier, R. *Biochim. Biophys. Acta* **2003**, *1606*, 147.

(22) Samuilov, V. D.; Borisov, A. Y.; Barskey, E. L.; Borisova, O. F.; Kitashov, A. V. *Biochem. Mol. Biol. Int.* **1998**, *46*, 333.

(23) Lee, J. W.; Zipfel, W.; Owens, T. G. *J. Fluo. Photochem. Yield* **1992**, *51*, 79.

(24) El-Khouly, M.; Araki, Y. F., M.; Watanabe, A.; Ito, O. *Photochem. Photobiol.* **2001**, *74*, 22.

(25) (a) Chen, S.; Ingram, R. S.; Hostetler, M. J.; Pietron, J. J.; Murray, R. W.; Schaaff, T. G.; Khoury, J. T.; Alvarez, M. M.; Whetten, R. L. *Science* **1998**, *280*, 2098. (b) Chen, S.; Murray, R. W. *J. Phys. Chem. B* **1999**, *103*, 9996. (c) Templeton, A. C.; Cliffel, D. E.; Murray, R. W. *J. Am. Chem. Soc.* **1999**, *121*, 7081. (d) Hicks, J. F.; Templeton, A. C.; Chen, S. W.; Sheran, K. M.; Jasti, R.; Murray, R. W.; Debord, J.; Schaaf, T. G.; Whetten, R. L. *Anal. Chem.* **1999**, *71*, 3703. (e) Hicks, J. F.; Zamborini, F. P.; Murray, R. W. *J. Phys. Chem. B* **2002**, *106*, 7751. (f) Templeton, A. C.; Wuelfing, W. P.; Murray, R. W. *Acc. Chem. Res.* **2000**, *33*, 27. (g) Aguila, A.; Murray, R. W. *Langmuir* **2000**, *16*, 5949.

(26) Baum, T.; Brust, M.; Bethell, D.; Schiffrin, D. J. *Langmuir* **1999**, *15*, 866.

(27) Fishelson, N.; Shkrob, I.; Lev, O.; Gun, J.; Modestov, A. D. *Langmuir* **2001**, *17*, 403.

(28) (a) Ipe, B. I.; George Thomas, K.; Barazzouk, S.; Hotchandani, S.; Kamat, P. V. *J. Phys. Chem. B* **2002**, *106*, 18. (b) Kamat, P. V.; Barazzouk, S.; Hotchandani, S. *Angew. Chem., Int. Ed.* **2002**, *41*, 2764. (c) Sudeep, P. K.; Ipe, B. I.; Thomas, K. G.; George, M. V.; Barazzouk, S.; Hotchandani, S.; Kamat, P. V. *Nano Lett.* **2002**, *2*, 29. (d) George Thomas, K.; Kamat, P. V. *Acc. Chem. Res.* **2003**, *36*, 888. (e) Chandrasekharan, N.; Kamat, P. V. *Nano Lett.* **2001**, *1*, 67. (f) Jakob, M.; Levanon, H.; Kamat, P. V. *Nano Lett.* **2003**, *3*, 353. (g) Subramanian, V.; Wolf, E. E.; Kamat, P. V. *J. Phys. Chem. B* **2001**, *105*, 11439. (h) Subramanian, V.; Wolf, E. E.; Kamat, P. V. *J. Am. Chem. Soc.* **2004**, *126*, 4943.

(29) (a) Brust, M.; Walker, M.; Bethell, D.; Schffrin, D. J.; Whyman, R. *J. Chem. Soc., Chem. Commun.* **1994**, 80. (b) Bethell, D.; Brust, M.; Schiffrin, D. J.; Kiely, C. *J. Electroanal. Chem.* **1996**, *409*, 137.

(30) Fitzmaurice, D.; Rao, S. N.; Preece, J. A.; Stoddart, J. F.; Wenger, S.; Zaccheroni, N. *Angew. Chem., Int. Ed.* **1999**, *38*, 1147.

(31) Imahori, H.; Norieda, H.; Yamada, H.; Nishimura, Y.; Yamazaki, I.; Sakata, Y.; Fukuzumi, S. *J. Am. Chem. Soc.* **2001**, *123*, 100.

(32) McConnel, W. P.; Novak, J. P.; Brousseau, L. C., III; Fuierer, R. R.; Tenent, R. C.; Feldheim, D. L. *J. Phys. Chem. B* **2000**, *104*, 8925.

(33) (a) Link, S.; El-Sayed, M. A. *J. Phys. Chem. B* **1999**, *103*, 4212. (b) Link, S.; Akihiro, F.; Mohamed, T. A.; Masuhara, H.; El-Sayed, M. A. *J. Phys. Chem. B* **2002**, *106*, 945.

(34) (a) Shipway, N. A.; Lahav, M.; Willner, I. *Adv. Mater.* **2000**, *12*, 993. (b) Shipway, N. A.; Lahav, M.; Gabai, R.; Willner, I. *Langmuir* **2000**, *16*, 8795. (c) Shipway, N. A.; Katz, E.; Willner, I. *ChemPhysChem* **2000**, *1*, 18. (d) Lahav, M.; Gabriel, T.; Shipway, A. N.; Willner, I. *J. Am. Chem. Soc.* **1999**, *121*, 258.

(35) Shenhar, R.; Rotello, V. M. *Acc. Chem. Res.* **2003**, *36*, 549.

(36) Rao, C. N. R.; Kulkarni, G. U.; John Thomas, P.; Edwards, P. P. *Chem. Eur. J.* **2002**, *8*, 29.

(37) (a) Wood, A.; Giersig, M.; Mulvaney, P. *J. Phys. Chem. B* **2001**, *105*, 8810. (b) Ung, T.; Dunstan, D.; Giersig, M.; Mulvaney, P. *Langmuir* **1997**, *13*, 1773.

(38) Avouris, P.; Persson, B. N. J. *J. Phys. Chem.* **1984**, *88*, 837.

(39) Rossetti, R.; Brus, L. E. *J. Phys. Chem.* **1982**, *76*, 1146.

(40) Drexhage, K. H.; Flock, M.; Kuhn, H.; Shafer, F. P.; Spurlig, W. *Ber. Bunsen-Ges. Phys. Chem.* **1969**, *73*, 1179.

(41) Dulkeith, E.; Morteani, A. C.; Niedereichcholz, T.; Klar, T. A.; Feldmann, J.; Levi, S. A.; van Veggel, F. C. J. M.; Reinhoudt, D. N.; Möller, M.; Gittins, D. I. *Phys. Rev. Lett.* **2002**, *89*, 203002.

(42) Fan, C.; Wang, S.; Hong, J. W.; Bazan, G. C.; Plaxco, K. W.; Heeger, A. J. *PNAS* **2003**, *100*, 6297.

(43) Nasr, C.; Kamat, P. V.; Hotchandani, S. *J. Phys. Chem. B* **1998**, *102*, 10047.

(44) Bedja, I.; Hotchandani, S.; Kamat, P. V. *J. Phys. Chem.* **1993**, *97*, 11064.

(45) Nagarajan, V.; Fessenden, R. W. *J. Phys. Chem.* **1985**, *89*, 2330.

(46) Hoff, A. J.; Amesz, J. In *Chlorophylls*; Scheer, H., Ed.; CRC Press: Boca Raton, FL, 1995; p 726.

(47) Lakowicz, J. R. *Principles of fluorescence spectroscopy*; Plenum Press: New York, 1993; chapter 9.

(48) Quinn, B. M.; Liljeroth, P.; Ruiz, V.; Laaksonen, T.; Kontturi, K. *J. Am. Chem. Soc.* **2003**, *125*, 6644.

(49) (a) Clarke, R. H.; Hotchandani, S.; Jagannathan, S. P.; Leblanc, R. M. *Photochem. Photobiol.* **1982**, *36*, 575. (b) Clarke, R. H.; Hotchandani, S.; Jagannathan, S. P.; Leblanc, R. M. *Chem. Phys. Lett.* **1982**, *89*, 37. (c) Hotchandani, S.; Leblanc, R. M.; Clarke, R. H.; Fragata, M. *Photochem. Photobiol.* **1982**, *36*, 235.

(50) Kooyman, R. P. H.; Schaafsma, T. J.; Kleibeuker, J. F. *Photochem. Photobiol.* **1977**, *26*, 235.

(51) Seely, G. R. *Photochem. Photobiol.* **1978**, *27*, 639.

(52) Livingston, R. *J. Am. Chem. Soc.* **1955**, *77*, 2179.

(53) Asano, M.; Koningstein, J. A. *Chem. Phys.* **1981**, *57*, 1.

(54) Kuwahara, Y.; Akiyama, T.; Yamada, S. *Langmuir* **2001**, *17*, 5714.